Detector for a Linear Collider

J. Mnich[a]*

[a]III. Phys. Inst. B, RWTH Aachen,
52056 Aachen, Germany

The proposals under discussion for a new e^+e^- Linear Collider with centre-of-mass energies around 1 TeV include designs for large detectors with unprecedented performances in energy, momentum and position resolution. These very stringent requirements are dictated by the precision measurements aimed at this collider to complement the exploratory experiments at the Large Hadron Collider. Here a status report on detector R&D projects for the Liner Collider is given focused on the technologies under study for the vertex detector, the large tracking chamber and the calorimeters.

1. Introduction

Today there is a general consensus among particle physicists that after the Large Hadron Collider (LHC) currently under construction at CERN the next large accelerator project should be a high luminosity electron-positron linear collider (LC) with a centre-of-mass (cms) energy in the 1 TeV range. Precision measurements would be possible in such an e^+e^--experiment which ideally complement the discoveries expected at the LHC and enlarge our understanding of particle physics at the TeV scale. Obvious examples are measurements of the properties of the Higgs boson and supersymmetric particles if they exist.

It is also desirable that the LC starts operation rather early after the start-up of the LHC which is expected in the year 2007. Interaction between the experimental groups based on their results could take place, exploiting the complementarity of the physics potential of the two machines at its best.

Several concepts for an 1 TeV LC are being developed for more than a decade now at different places in the world. Very impressive progress has been made over the last years and today there is already one design available which has proven its feasibility. Therefore the technology for a LC at 1 TeV is in hand and the project is now subject to financial and political discussions.

The experimental goals defined for this e^+e^--experiment require very challenging performances of the detector to fully exploit the advantages of an electron-positron collider with respect to a proton machine. For this reason worldwide studies are going on to investigate the use of most modern detector technologies and to verify that the required performances can be obtained. An overview of current trends and the status of this R&D program is given below.

2. Overview on Linear Collider Projects

The construction of the LC poses several very demanding technological challenges. Three projects are being investigated by laboratories and physicist in different regions of the world:

- The Tera Electron volt Superconducting Linear Accelerator (TESLA) [1] proposed by an international collaboration formed around DESY in Europe;
- the Next Linear Collider (NLC) in America;
- the Japanese Linear Collider (JLC) in Asia.

These designs include cms energies between 0.5 TeV and 1 TeV and high luminosities in the range of $3 \cdot 10^{34}/\mathrm{cm}^2/\mathrm{s}$. The latter figure is more than two orders of magnitude larger than the peak luminosity achieved at LEP and four orders

*supported by the German Bundesministerium für Bildung und Forschung

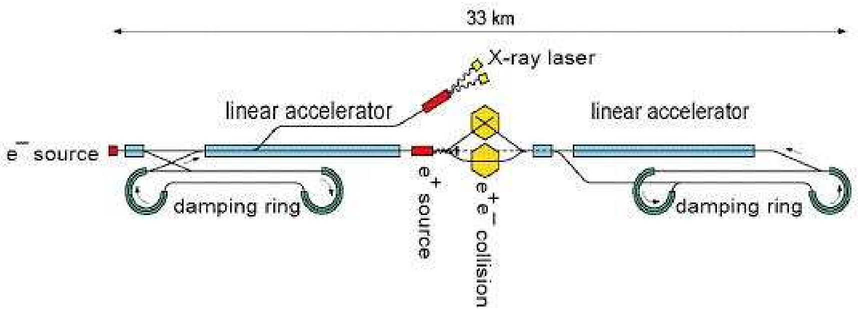

Figure 1. Layout of the proposed TESLA e^+e^- Linear Collider. The project includes a free electron X-ray laser [1].

of magnitude larger than at SLC which can be considered as a prototype LC. In all projects the construction of tunnels of about 30 km length is considered, i.e. of similar size as LEP. The accelerating cavities need gradients between 23 MV/m and 50 MV/m to reach the required collision energy which should be compared to the gradient of 7 MeV/m reached at LEP.

The main difference between the three concepts is that the TESLA design is based on the use of superconductive cavities whereas NLC and JLC envisage beam acceleration by warm cavities. Also the frequency of the accelerating electromagnetic wave at TESLA is lower (1.3 GHz) as compared to the other design (5.7 GHz or 11.4 GHz). As a consequence the geometrical size of the accelerating structures at TESLA is larger which entails somewhat less strict requirements on alignment and beam sizes at the interaction point.

A fourth design project, CLIC [2] at CERN, could open in a more distant future the route to even higher energies up to 5 TeV. Here low energy, but high current, drive beams are used to accelerate electrons with a gradient of 150 MV/m.

Among the projects under discussion the TESLA concept is certainly the most advanced one. A Technical Design Report [1] has been presented by the TESLA collaboration in spring 2001. The proposed layout of the TESLA collider is shown in Figure 1. It is proposed that this accelerator should be build in the north of Germany connected to the DESY site at Hamburg.

One of the most critical items of this project is to demonstrate the feasibility of the concept and the performance of the superconductive cavities. Recently industrially produced nine-cell cavity modules reached an accelerating gradient of 35 MV/m (Figure 2) which is the value required for a cms energy of 800 GeV.

Another important issue is the strong focusing of the two beams at the interaction point necessary to achieve the desired high luminosity. Experiments at SLAC have demonstrated that the necessary horizontal and vertical beam sizes of $\sigma_x^* = 553$ nm and $\sigma_y^* = 5$ nm are in reach for TESLA beam energies [4]. The second part of the luminosity problem is that the two small beams can be made colliding head-on which is so far only supported by detailed simulations.

Because this accelerator project is in a rather advanced technical state TESLA is used as the example in the following discussions on the LC physics and the detector design.

3. Physics at the e^+e^- Linear Collider

In order to appreciate the physics goals set for the experiments at the LC it is important to note that at the time this accelerator starts operation the LHC will have been running al-

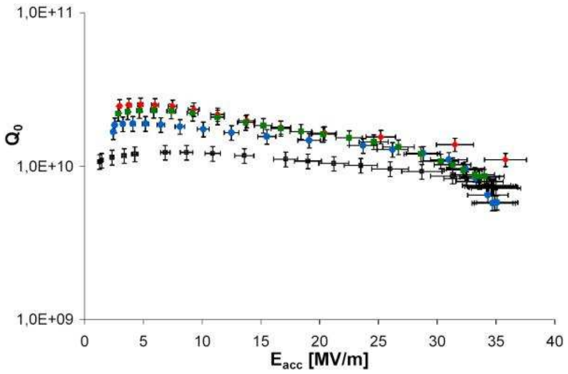

Figure 2. The quality factor measured as a function of the accelerating gradient for several prototype nine-cell superconductive cavity modules of TESLA. For all devices a gradient of 35 MV/m is reached before the quality factor drops below the critical value [3].

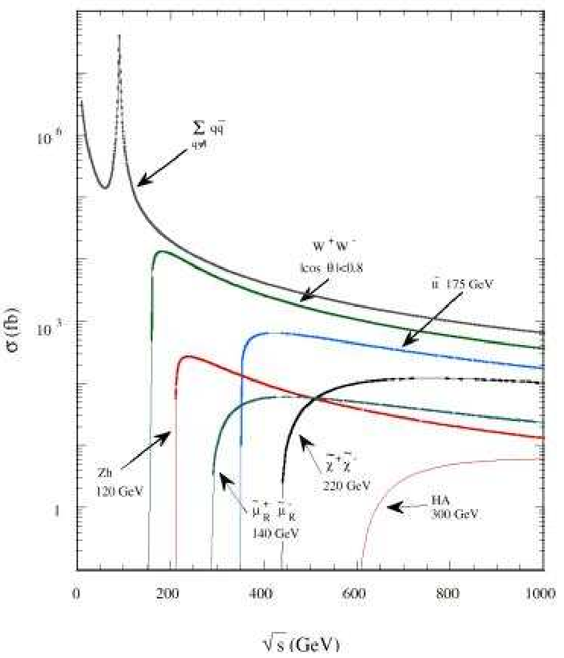

Figure 3. Comparison of cross sections Standard Model and MSSM processes up to a cms energy of 1 TeV.

ready for several years. Thus major discoveries to be made in the energy range up to 1 TeV will most likely have been achieved already in proton-proton collisions. For instance, if the Higgs boson and supersymmetric particles exist the LHC experiments will have observed them. Hence, the rôle of the LC is to complement the initial particle discoveries by precision measurements of their properties exploiting the unique features of e^+e^--experiments: the cleanness of the experimental environment and the well defined kinematic of the colliding particles. A few striking examples are given in this section. The cross sections of various Standard Model reactions and some processes predicted by the Minimal Supersymmetric Model (MSSM) are shown in Figure 3.

The $1/E^2$ behavior of s-channel processes reduces the cross sections at the LC by about an order of magnitude as compared to the situation at the highest LEP energies. However, this is more than compensated by the expected high luminosity resulting in high event rates even for rare processes. For example, if the Higgs boson is as light as indicated by the results obtained at LEP [5] about 1000 Higgs events per year would be observed at the LC. This is similar to the number of W-pair events collected at LEP per year and experiment therefore permitting studies of the Higgs properties to a precision comparable to our current knowledge of the W boson.

The Higgsstrahlung process, depicted in Figure 4, together with the high event rates offers a possibility to detect the Higgs boson without making any assumptions on its decay and hence its couplings to other particles. The production of the Higgs is revealed by the presence of a real Z boson in the final state which can be identified by the invariant mass of its decay products. The easiest case are Z boson decays into electron and muon pairs. Figure 5 shows the expected recoil mass distribution obtained from the measured momentum of muon pairs in such events.

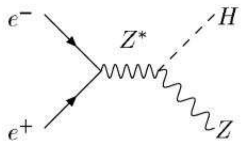

Figure 4. Production of the Higgs boson through the Higgsstrahlung process.

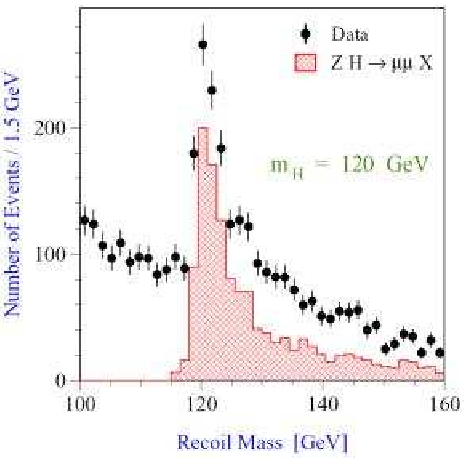

Figure 5. Recoil mass distribution in simulated $\mathrm{e}^+\mathrm{e}^- \to \mathrm{HZ} \to X + \mu^+\mu^-$ events, including background.

This distribution can be used to identify Higgs bosons and to measure the mass.

The analysis of the Higgs decay products in these events provides a straightforward and largely unbiased measurement of the Higgs branching ratios and therefore its couplings to other particles. The expected experimental precision for different Higgs masses is illustrated in Figure 6. This consists a very important test of the Standard Model as it actually verifies the rôle of the Higgs boson.

The spin and parity quantum numbers of the

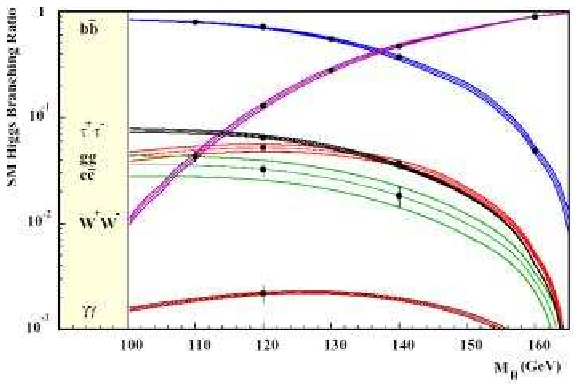

Figure 6. Expected experimental precision on the measurement of Higgs branching ratios. The curves show the Standard Model calculations as a function of the Higgs mass including their uncertainties.

Higgs can easily be determined in an energy scan at the production threshold. Figure 7 demonstrates that the Standard Model value $J = 0$ can be unambiguously verified using a total luminosity of only 20 fb^{-1} which can be collected in about half a year of operation.

Another important measurement in the Higgs sector only possible at the LC is the verification of the Higgs potential which would experimentally confirm the concept of spontaneous symmetry breaking. In the Standard Model the Higgs potential $V(H)$ expanded around the vacuum expectation value $v = \sqrt{-\mu^2/\lambda}$ can be written as

$$V(H) = \lambda v^2 H^2 + \lambda v H^3 + \frac{1}{4}\lambda H^4 \qquad (1)$$

with the free parameters $\mu^2 < 0$ and $\lambda > 0$. As the first term represents the Higgs boson mass, $m_{\mathrm{H}} = \sqrt{2\lambda}\, v$, the second and third imply the existence of triple and quartic Higgs boson vertices, parametrized by the coupling constants g_{HHH} and g_{HHHH}. At TESLA the existence of the triple Higgs boson vertex can be established by the study of double Higgsstrahlung events (Figure 8) and the parameter g_{HHH} will be measured to a precision of about 20%. Even though the con-

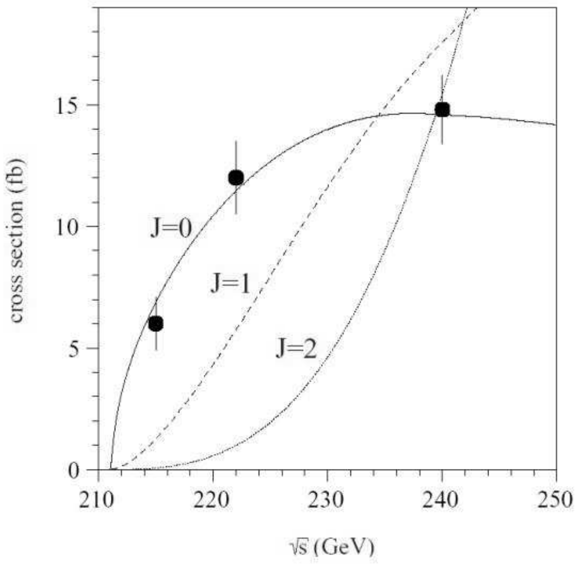

Figure 7. Determination of the spin J of the Higgs boson from an energy scan at the production threshold. Shown are curves of cross sections as a function of the cms energy for three hypotheses together with the expected experimental errors ($J = 0$) for a total of 20 fb^{-1}.

firmation of the last term in Equation 1 is not possible this measurement would be a major step forward in unveiling the nature of mass generation.

As a last example to demonstrate the capabilities of the LC we briefly mention Supersymmetry (SUSY). If supersymmetric particles with masses below approximately 2 TeV exist they will be discovered at the LHC and SUSY will be the new Standard Model at the time the LC starts up. However, as most likely a variety of SUSY particles with similar properties will be produced simultaneously this would pose severe problems for the LHC experiments to disentangle different final states.

Here the conditions at the LC are much more favourable. SUSY particles can easily be produced separately and distinguished by their mass

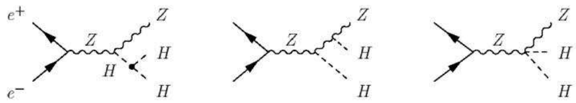

Figure 8. Feynman diagrams of double Higgs boson production at the LC. The left diagram is sensitive to the triple Higgs boson vertex and the coupling constant g_{HHH}.

through adjustments of the cms energy. Such threshold scans will also provide precise mass measurements of all SUSY particles kinematically accessible.

Another important experimental tool at the LC is the polarization of electrons and positrons. Also this way a separation of SUSY partners can be obtained, e.g $\mathrm{e}^+_\mathrm{L}\mathrm{e}^-_\mathrm{L} \to \tilde{\mathrm{e}}^+_\mathrm{L}\tilde{\mathrm{e}}^-_\mathrm{L}$ versus $\mathrm{e}^+_\mathrm{R}\mathrm{e}^-_\mathrm{R} \to \tilde{\mathrm{e}}^+_\mathrm{R}\tilde{\mathrm{e}}^-_\mathrm{R}$. and the determination of the properties of SUSY particles is facilitated.

4. Implications for the Detector Design

The physics goals for an LC as outlined above and the design parameters of the accelerator have large implications on the concept for the detector. With respect to LEP more complex final states are expected. As an example we recall the important double Higgs productions $\mathrm{e}^+\mathrm{e}^- \to \mathrm{ZHH} \to$ 6 jets/leptons and the production of charged Higgs bosons $\mathrm{e}^+\mathrm{e}^- \to \mathrm{H}^+\mathrm{H}^- \to \bar{\mathrm{t}}\mathrm{b}\,\mathrm{t}\bar{\mathrm{b}} \to$ 8 jets as expected in SUSY. As compared to previous and existing $\mathrm{e}^+\mathrm{e}^-$-detectors higher energies and a wider range of particle energies – from GeV to TeV – must be measured. The higher energy also causes a larger Lorentz boost leading to higher particle densities in jets.

The are other important detector design issues caused by differences between linear and circular $\mathrm{e}^+\mathrm{e}^-$-colliders. At the LC there will be much higher background at the interaction point which is mostly created by beam strahlung produced through electromagnetic interactions between the strongly focused electron and positron beams.

The largely different time structure of the collisions implies consequences for the detector readout speed and the trigger system. Contrary to circular e^+e^--colliders with constant time intervals between collisions the LC will not have equally spaced particle bunches. For instance the TESLA design[2] foresees trains containing 2820 bunches separated by 337 ns time intervals. These trains are repeated five times per second. Using large front end buffers, and provided that the occupancy during a bunch train can be kept low, the long gap between trains can be used to read out the detector. This renders unnecessary a sophisticated first level trigger.

However, the most important consideration driving the design of the detector is to achieve the best possible energy, momentum and vertex resolutions. Consider for example the unbiased detection of the Higgs boson which relies on the reconstruction of the leptonic Z decays: $Z \to e^+e^-$ and $Z \to \mu^+\mu^-$ (Figure 5). Improved momentum resolution directly translates into better efficiency and lower background and thus governs the experimental performance. Likewise, the identification of the b- and c-quarks in the Higgs decay requires the best possible reconstruction of primary and secondary vertices.

Another important reason to aim for the best possible energy resolution is the search for SUSY particles. Here the most prominent experimental sign[3] is the missing energy carried away by the invisible lightest SUSY particle which is in most scenarios the lightest neutralino $\tilde{\chi}_0$. The detection of missing energy signatures and hence the quality of SUSY searches is determined by the hermeticity of the detector and its energy resolution.

Here the concept of a detector as described in the TESLA technical design report [1] is discussed. Figure 9 shows a sketch of one quadrant of the detector. Going form the interaction point outwards the key elements of the design are a silicon pixel vertex detector, a large Time Projection Chamber (TPC), the electromagnetic and the hadronic calorimeters and a muon detector. The central part of the detector is placed in a

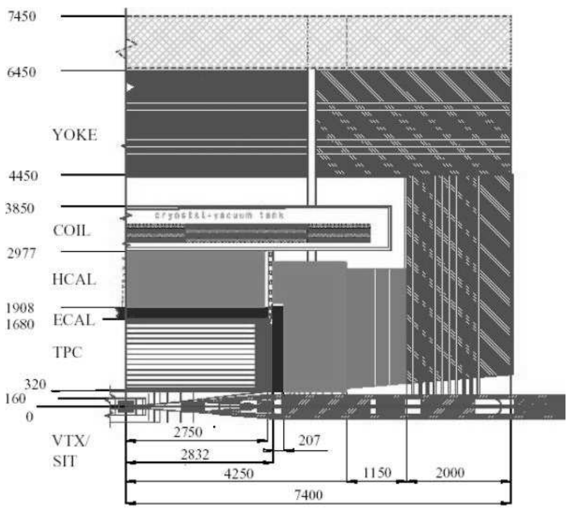

Figure 9. The concept of the TESLA detector. Shown is a sketch of the right upper quadrant of the design.

solenoidial magnetic field of 4 T provided by a superconductive magnet. In order not to compromise the energy measurement both coil and return yoke of the magnet are outside the hadron calorimeter.

In the following sections we describe several design options and considerations for the silicon pixel vertex detector, the TPC and the calorimeters.

5. Vertex Detector

The main goals of this detector part is the precise reconstruction of primary and secondary event vertices to identify b- and c-quarks as well as τ-leptons. In particular, for the measurement of Higgs boson branching ratios the best possible efficiency and background suppression is desirable. Note that the higher cms energy does not help to identify long lived particles as smaller decay angles compensate the larger decay length. For instance, the average impact parameter for b-hadrons is 300 μm for $\beta\gamma > 3$ independent of the

[2] These figures apply for the 500 GeV cms energy layout.
[3] This holds for models which conserve R-parity.

Table 1
Comparison of parameters of the silicon pixel vertex detectors of the TESLA detector design and the SLD experiment.

	TESLA	SLD
Inner radius	15 mm	28 mm
Single point resolution	$< 5\ \mu$m	8 μm
Material per layer	0.06% X_0	0.4% X_0
Total material budget	$< 1\%\ X_0$	

cms energy. Improvements can only be achieved from advanced detector designs.

The objective for the impact parameter resolution is

$$\delta(\mathrm{IP}) \leq 5\ \mu\mathrm{m} \oplus 10\ \mu\mathrm{m}/(p \sin^{3/2}\theta) \qquad (2)$$

where the first term originates from the intrinsic detector resolution and second term from multiple scattering in the device which depends on the scattering angle θ and the momentum p (in GeV). Note that the latter consists a significant improvement with respect to the performance achieved with the SLD vertex detector: $\delta(\mathrm{IP}) \leq 8\ \mu\mathrm{m} \oplus 33\ \mu\mathrm{m}/(p \sin^{3/2}\theta)$ [6].

The baseline design for the vertex detector consist of five layers of thin silicon pixel detectors which will allow for a stand alone tracking and the internal calibration of the device. Some parameters are listed in Table 1 and compared to the SLD experiment.

The three main design issues which drive the R&D efforts for this detector are a low material budget, radiation hardness and the readout speed. The goal is to reduce the material per layer to 0.06% of a radiation length X_0 which corresponds to 60 μm of silicon. To minimize the total amount of material the support structure must be optimized. One scheme under study (Figure 10) avoids direct support of the silicon by applying moderate stress to the detectors using springs.

Due to the much higher background levels as compared to previous e^+e^--experiments radiation hardness is an issue for the design of the vertex detector. However, the expected doses at TESLA are still much below the doses the LHC experiments will have to cope with (Table 2).

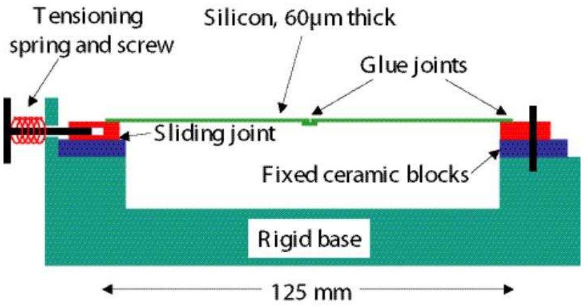

Figure 10. Model for the mechanical support of thin silicon pixel detector.

Table 2
Comparison of expected radiation doses at TESLA and the CMS detector at LHC [7] after 10 years of operation for the innermost layer of the vertex detector.

	TESLA $r_i = 1.5$ cm	CMS $r_i = 4.3$ cm
Dose (γ, e, $h^\pm$)	10 kGy	1000 kGy
Neutron (1 MeV)	$10^{10}/\mathrm{cm}^2$	$10^{15}/\mathrm{cm}^2$

Therefore it is safe to assume that the problem of radiation hardness can be solved with current technologies.

A more critical issue is to avoid integration of the large background during the long bunch trains. The average occupancy of the channels must be kept below a few percent to ensure pattern recognition capability. This requires a small pixel size of the order of 20 μm $\times$ 20 μm resulting in a total number of about 800 million pixels. In addition, the detector has to be read out at least 10 times during the 1 ms duration of a bunch train which implies a rather large improvement in speed as compared to pixel detectors used so far in e^+e^--experiments.

Currently three different detector technologies for the vertex detector are under investigation:

1. Charge Coupled Device (CCD),

2. DEPleted Field Effect Transistor (DEPFET)
3. and CMOS Monolithic Active Pixel Detector (MAPS).

The CCD technology is now widely used by industry for many consumer products. Also large CCD detectors have been build for high energy experiments like the SLD vertex detector with 300 million pixels. Features like a coordinate precision below 5 μm and low power consumption have been demonstrated.

The biggest obstacle left for the use in an LC vertex detector is the slow readout speed [8]. In currently available CCD detectors the charge liberated in a pixel is shifted first to the end of the column of the pixel matrix and then along the row to a pre-amplifier. This fully serial readout of large pixel areas limits the readout speed. To match the requirements at the LC this scheme must be changed such that the columns of the pixel matrix are read out in parallel. Such CCD cameras with parallel readout have been developed already and are used for example in X-ray astronomy.

Another promising candidate for the vertex detector is the DEPFET technology [9]. The detector consists of fully depleted sensors with an integrated pre-amplifier for each pixel. The advantages are low power consumption and very low noise (10 e$^-$) at room temperature. Thinning of the detectors to 50 μm seems possible. But also here the required readout speed needs further developments.

Figure 11 shows a prototype DEPFET detector consisting of 50 μm $\times$ 50 μm pixels [10]. A resolution of 9 μm as been achieved with this device.

The most recent developments are MAPS detectors which are based on standard CMOS wafers which integrate all functions [11]. Since sensor and electronics are on the same wafer micro bonding becomes obsolete. Very small pixel sizes are achievable in this technology which has also proven its radiation hardness. Besides readout speed power dissipation might be an issue. However, the latter could be significantly reduced by exploiting the train structure of the collisions at the LC and pulsing the low voltage supply.

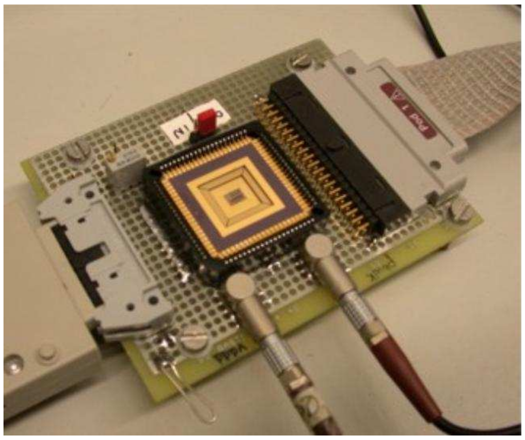

Figure 11. Picture of a prototype DEPFET pixel detector.

6. Tracking Detector

The rôle of the tracking detector is the precise measurement of charged particle momenta. As most prominent example we recall the importance for the Higgsstrahlung process as described in Section 3. Efficiency and background suppression directly profits from momentum resolution and in the ideal case the recoil mass resolution (Figure 5) would be limited by the total width of the Z boson.

In SUSY analyses the determination of the mass of scalar leptons can be performed from the end points of the momentum spectra in the decay $\tilde{\ell}^{\pm} \rightarrow \ell^{\pm} + \chi_0 \quad (\ell = \mathrm{e}, \mu)$ of which Figure 12 shows an example. The precision depends directly on the momentum resolution of the tracking system. Finally it is important to note that in the concept of the TESLA detector design the precise measurement of charged particles in jets by the tracking system is crucial for the jet energy measurement (see Section 7). From these and other considerations the goal for the momentum resolution of the full tracking system is set to be

$$\delta(1/p_{\mathrm{T}}) < 5 \cdot 10^{-5}\ \mathrm{GeV}^{-1}.$$

In addition, the tracking detector plays an impor-

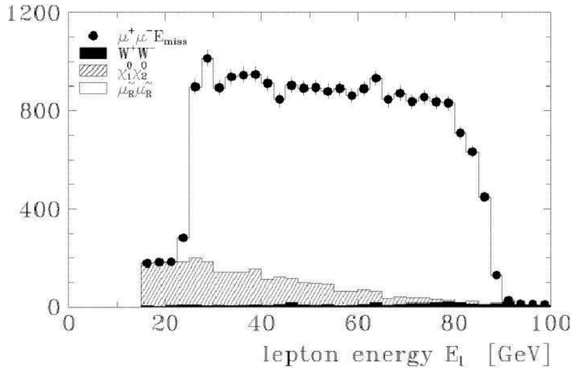

Figure 12. Simulation of the measured lepton spectrum in the decay of scalar muons $\tilde{\mu}^{\pm} \rightarrow \mu^{\pm} + \chi_0$.

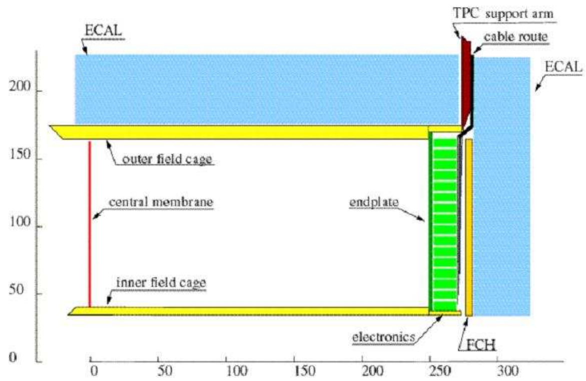

Figure 13. Proposed layout of the TPC.

tant rôle in particle identification and hence the specific ionization $\mathrm{d}E/\mathrm{d}x$ must be measured to better than 5%.

Most of the groups working on LC detector design believe that a large gas chamber, in particular of the TPC type, traditionally used in e^+e^--experiments is the most promising choice for the tracking detector. Large silicon based tracking detectors similar to the ones being constructed for the LHC experiments ATLAS [12] and CMS [7] are also studied. However, the much lower collision and particle rates at the LC compared to the LHC do not mandatorily require the use of fast silicon detectors. And a clear advantage of gaseous detectors is that, including all necessary infrastructure, they can be build with much less material as compared to silicon detectors, hence offering an obvious option to achieve the ambitious goal of very low material budget.

In the TESLA design the main tracking detector consists of a TPC of 5 m length and 3.5 m diameter. The layout of one quadrant shown in Figure 13. The goal on the total radiation length is $\leq 3\%~X_0$ in the barrel region and $\leq 30\%~X_0$ in the endcap region where the gas amplification takes place and the front-end electronic as well as other infrastructure reside.

To achieve the goals on momentum and double track resolution the tracks are measured with about 200 three-dimensional points each giving 100 μm single point resolution in the bending direction. The necessary single point resolution constitutes a tenfold improvement compared to the performance achieved with a TPC at LEP. Clearly a new concept for the gas amplification is needed to replace the classical method of proportional wires.

Micro pattern gas detectors like Gas Electron Multiplier (GEM) foils [13] or Micromegas [14] offer possible solutions. The much finer granularity of these detectors permits smaller readout pads and the two-dimensional symmetry minimizes systematic perturbations from $\vec{E} \times \vec{B}$ effects. Other common features of both detectors types are that only the fast electron signal is detected and that ion feedback from the gas amplification into the large chamber volume is intrinsically suppressed.

A typical GEM structure is shown in Figure 14. In a capton foil of 50 μm thickness coated with thin layers of copper holes of 75 μm diameter are etched with a pitch of 140 μm. A moderate voltage of a few hundred volts applied between the two electrodes creates an electric field in the holes large enough for gas amplification. Stable operation with a total amplification of 10^4

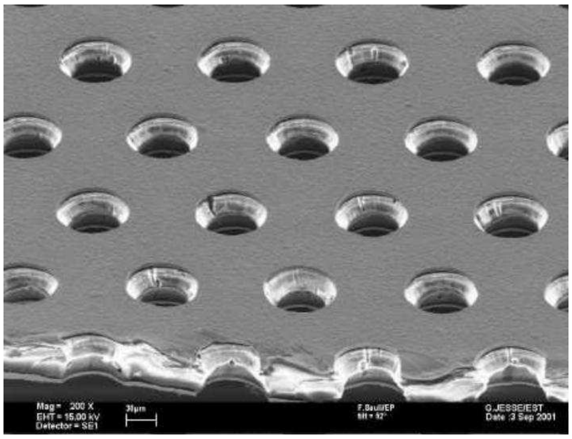

Figure 14. Photograph showing the typical structure of a GEM foil.

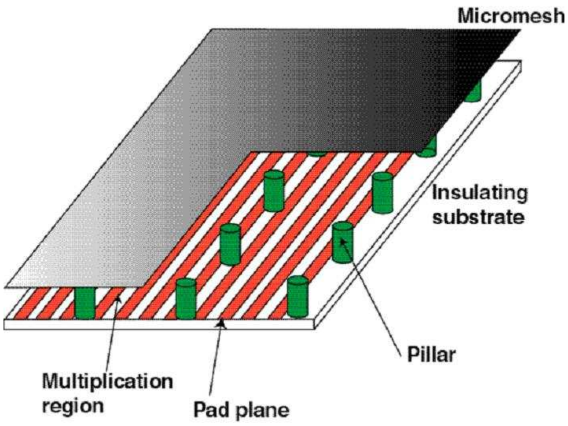

Figure 15. Sketch of a typical Micromegas structure.

can be achieved by staggering two or three GEM foils and subdividing the amplification in several steps [15]. An example for this technique has been realized by the COMPASS experiment [16].

Micromegas detectors are asymmetric parallel plate chambers with micromesh of typically 50 μm pitch (Figure 15). Their operation is based on the saturation of the Townsend coefficient at high electric fields such that the gas amplification is largely independent from variations in the gap.

In both detector types the electron signal is collected on small pads. As the transverse dimension of the electron cloud is much smaller than the induced signal from proportional wires (Figure 16) the signal is not always spread over several pads disabling the improvement of the spatial resolution through the determination of the centre-of-gravity of the electron cloud.

A possible solution is evidently a reduction of the pad size to the expense of a drastically increase of the number of readout channels. Under investigation is the replacement of the pads by the bump bonds of readout chips used for pixel detectors. More classical solutions to this problem are capacitive or resistive couplings between adjacent pads to split the signal as well as alternative pad geometries like chevron shapes.

7. Calorimeter

To exploit the missing energy signature of SUSY best possible hermeticity is an important design goal for the calorimeter. For this reason the magnet coil is placed outside the calorimeter. Fast readout and good time resolution is required to avoid event pile up. However, the most challenging goal is the excellent energy and angular resolution for electrons and photons but also for hadronic jets. To distinguish hadronic W- and Z-decays the jet energies must be measured with a resolution of $\sigma_E = 30\%/\sqrt{E}$.

The way to achieve this ambitious goal is to measure energy or momentum separately for every particle in a jet [17,18]. On average about 60% of the jet energy is carried by charged particles which can be precisely measured in the tracker. Photons carry 30% of the jet energy which can be measured relatively accurate in the electromagnetic part of the calorimeter such that only the measurement of the small fraction of neutral hadron in the jet suffers from the large fluctuations in hadronic interactions. The envisaged strategy for the jet energy measurement extends the energy flow algorithms used at LEP to particle reconstruction.

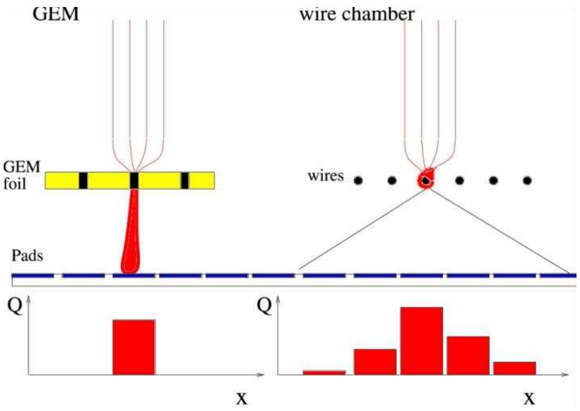

Figure 16. Sketch of the pad readout: the small size of the electron signal from GEM foils is compared to the wide induction signal from proportional wires.

This technique requires a highly granular calorimeter which is illustrated in Figure 17. The longitudinal segmentation of the electromagnetic part should be of the order of a radiation length X_0 and the required transversal segmentation is given by the Moliere radius r_M which should be small. A silicon-tungsten calorimeter ($r_M = 9$ mm) is a natural choice and a possible layout is shown in Figure 18. The structure consists of 40 layers of tungsten plates interleaved with silicon wafers which are segmented into pads of 1 cm^2. The expected energy resolution is

$$\Delta E/E < 0.1/\sqrt{E/\mathrm{GeV}}.$$

This design requires about 2000 m^2 total area of silicon which is an order magnitude more than the size of the CMS silicon tracker currently under construction. Because of the large quantity of silicon needed this option for the electromagnetic calorimeter is rather expensive. The performance of such a calorimeter must be still demonstrated in a larger scale experiment.

Alternatively a lead calorimeter with scintillating fibre readout is under consideration. This design has a coarser transversal granularity of the order of 5 cm $\times$ 5 cm but the advantage that the same design and components can be used for the hadron calorimeter. The challenge here consists in the readout of the fibres in the 4 T magnetic field and to achieve a sufficient light yield. Various geometries of fibre tiles are being studied. Figure 19 shows the design.

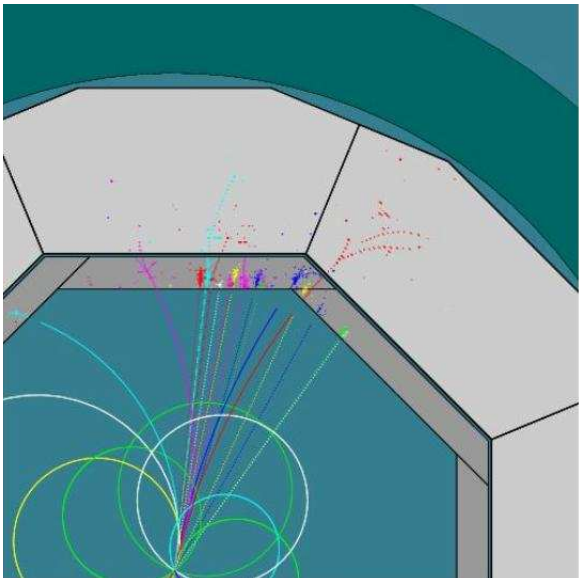

Figure 17. Simulation of a hadronic jet in the highly granular calorimeter proposed for the TESLA detector.

In addition the feasibility of a digital hadron calorimeter is investigated. The readout is highly segmented with pads of 1 cm^2 which are evaluated only binary: hit or no hit. This could simplify enormously the front-end electronic making the large number of channels feasible. Resistive plate chambers and small wire cambers are candidate detectors.

8. Summary and Outlook

The precision measurements aimed at the e$^+$e$^-$ Linear Collider set very high demands on the performance of the detector. A detector similar to the ones used at LEP or SLC is clearly not suf-

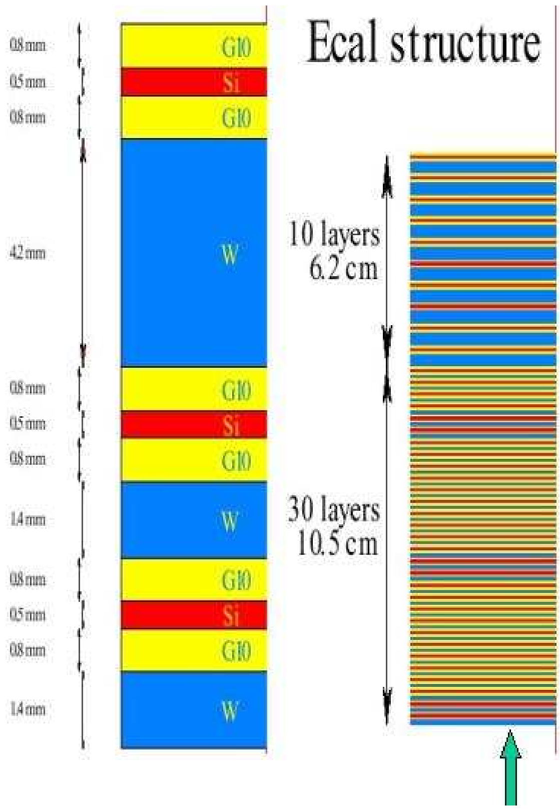

Figure 18. Layout of the electromagnetic calorimeter.

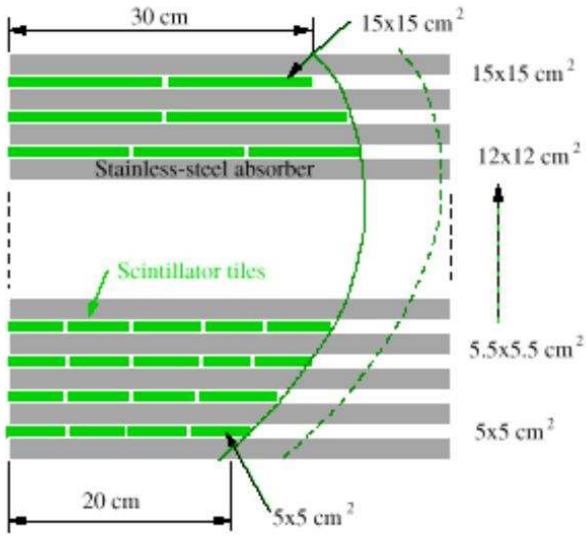

Figure 19. Layout of the lead – scintillating fibre calorimeter.

ficient. Instead the use of modern state-of-the-art technologies is required to achieve the performance necessary to fully exploit the physics potential of e^+e^--collisions at 1 TeV cms energy.

To find and investigate technologies suited for this detector a number of world wide R&D projects have started. Examples are the TPC group [19] and the CALICE collaboration [20] which studies the various options for the calorimeter. An international board [21] is coordinating the world wide activities and defining common goals. In Europe, the ECFA/DESY [22] study provides the framework for physics and detector development studies.

It is very clear that the R&D effort must be extended in future to achieve the ambitious goals and to have a working detector ready for the exciting physics at the Linear Collider.

Acknowledgments

I would like to thank the organizers of this seminar for their invitation and their hospitality. I am indebted to many colleagues from the various Linear Collider R&D groups who provided and explained to me the results of their work. In particular, I am very grateful to S. Roth for the careful reading of the manuscript.

REFERENCES

1. TESLA Technical Design Report, DESY 2001-011 and ECFA 2001-209, Publisher: Deutsches Elektronen-Synchrotron DESY, Hamburg, Germany. `http://tesla.desy.de/new_pages/TDR_CD/start.html`.
2. A 3 TeV e^+e^- Linear Collider based on CLIC

Technology, CERN 2000-008,
http://ps-div.web.cern.ch/ps-div/CLIC
3. L. Lilje (DESY), private communication.
4. V. Balakin et al., Phys. Rev. Lett. 74, (1995), 2479;
http://www-project.slac.stanford.edu/nlc/testfac/FFTB.html.
5. The LEP Collaborations ALEPH, DELPHI, L3, OPAL, the LEP Electroweak Working Group and the SLD Heavy Flavour Group, CERN-EP/2002-091 and hep-ex/0212036; Search for the Standard Model Higgs Boson at LEP, The LEP Collaborations ALEPH, DELPHI, L3, OPAL and the LEP Working Group for Higgs Boson Searches, in preparation.
6. K. Abe et al., Nucl. Instr. and Meth. A 400 (1997) 287.
7. CMS Tracker Technical Design Report, CERN/LHCC 98-6 (1998).
8. A CCD-based vertex detector for TESLA, C. Damerell, ECFA/DESY Linear Collider Note 2001-023;
http://www.desy.de/~lcnotes/.
9. J. Kemmer and G. Lutz, Nucl. Instr. and Meth. A 253 (1987) 356.
10. A DEPFET based pixel vertex detector for the detector at TESLA, P. Fischer et al., ECFA/DESY Linear Collider Note 2002-004.
11. A CMOS based VTX detector, M. Winter et al., ECFA/DESY Linear Collider Note 2001-017.
12. ATLAS TDR 4, CERN/LHCC/97-16 (1997), ISBN 92-9083-102-2.
13. F. Sauli, Nucl. Instr. and Meth. A 386 (1997) 531.
14. Y. Giomataris et ad., Hurl. Instr. and Meth. A 376 (1996) 29.
15. M. Killenberg et al., Nucl. Instr. and Meth. A 498 (2003) 369.
16. The COMPASS experiment at CERN,
http://wwwcompass.cern.ch/.
17. J.C. Brient and H. Videau, The calorimetry at the future e^+e^- linear collider, Summer Study on the Future of Particle Physics, Snowmass 2001, hep-ex 0202004.
18. J. Cvach, Calorimetry at a future e+ e- collider, 31st International Conference on High Enery Physics, Amsterdam, July 2002, to appear in the proceedings.
19. http://alephwww.mppmu.mpg.de/~settles/tpc/welcome3.html.
20. http://polywww.in2p3.fr/tesla/calice.html.
21. Linear Collider Detector R&D, eds. J. Brau et al.,
http://blueox.uoregon.edu/~lc/randd.pdf.
22. Extended Joint ECFA/DESY Study on Physics and Detectors for a Linear Electron-Positron Collider,
http://www.desy.de/conferences/ecfa-desy-lcext.html.